

# Silver-Nanoparticle-Attached Indium Tin Oxide Surfaces Fabricated by a Seed-Mediated Growth Approach

Gang Chang,<sup>†</sup> Jingdong Zhang,<sup>‡,§</sup> Munetaka Oyama,<sup>\*,‡</sup> and Kazuyuki Hirao<sup>†</sup>

Department of Material Chemistry, Graduate School of Engineering, Kyoto University, Nishikyo-ku, Kyoto 615-8510, Japan, and Division of Research Initiatives, International Innovation Center, Kyoto University, Sakyo-ku, Kyoto 606-8501, Japan

Received: July 27, 2004; In Final Form: October 21, 2004

By applying a seed-mediated growth method that had been reported for the chemical synthesis of Ag nanorods and nanowires in aqueous solution, we successfully attached Ag nanosphere and nanorod particles to indium tin oxide (ITO) surfaces. In this method, it is characteristic that the attachment can be performed without using bridging reagents, such as 3-mercaptopropyltrimethoxysilane, but rather through a two-step immersion into the seed solution first and then into the growth solution containing AgNO<sub>3</sub>, cetyltrimethylammonium bromide, and ascorbic acid. It was found that the formed nanostructures were very sensitive to the amount of ascorbic acid in the growth solution. Whereas Ag nanoparticles grew on the ITO surface with a moderate dispersion when the concentration of ascorbic acid in the growth solution was 0.64 mM, the formation of nanorods and nanowires was observed when the ascorbic acid concentration was increased to 0.86 mM. The attachment of Ag nanoparticles onto the ITO surfaces was strong enough for further use, e.g., as a working electrode. From electrochemical measurements, it was confirmed that the outer spheres of the Ag nanoparticles involved in the redox reaction show the typical oxidation and reduction waves of Ag. In addition, the redox behavior of [Fe(CN)<sub>6</sub>]<sup>3-</sup>/[Fe(CN)<sub>6</sub>]<sup>4-</sup> was improved on the Ag-nanoparticle-attached ITO (AgNP/ITO) electrode, reflecting the low electron-transfer resistivity, which is a remarkable advantage of the present fabrication without using bridging reagents. This result indicated that the Ag nanoparticles promote the electron-transfer reactions by being present on the conducting ITO surface. The AgNP/ITO electrode was examined for the reduction of the methyl viologen dication in order to discuss some features of the present fabrication.

## Introduction

The shape and size of metal nanoparticles are known to affect their unique optical, electronic, and magnetic properties. Recently, much attention has been directed toward the fabrication of nanoparticles having various shapes and sizes by different methods. For Ag nanoparticles, shape-controlled synthetic methods have been actively studied; for example, nanocubes,<sup>1</sup> nanorods,<sup>2,3</sup> and nanowires<sup>2–5</sup> have been synthesized, and the synthesis of nanospheres has been developed.<sup>6,7</sup>

As the characteristic application of Ag nanoparticles, the surfaces on which Ag nanoparticles are dispersed can be utilized as substrates to activate surface-enhanced Raman scattering (SERS). Instead of electrochemically roughened Ag electrode surfaces, which is the normal substrate for observing SERS, Ag-nanoparticle-attached surfaces were fabricated to observe SERS signals using bridging reagents, such as 3-mercaptopropyltrimethoxysilane (MPTMS).<sup>8,9</sup> Natan and co-workers studied Ag colloid self-assembly onto organosilane-functionalized glass, carbon, and Au surfaces<sup>10</sup> and reported an improvement in heterogeneous electron transfer to [Ru(NH<sub>3</sub>)<sub>6</sub>]<sup>3+</sup> on the Ag-colloid-attached carbon, in addition to the SERS responses. Moreover, single Ag nanoparticles have recently been used as optical sensors by observing the localized surface plasmon resonance.<sup>11</sup>

As recognized from these examples, Ag-nanoparticle-attached surfaces are significant for improving optical and electrochemical measurements as well as potential applications as catalytic and electrocatalytic materials.<sup>12,13</sup> Thus, the methods of attaching Ag nanoparticles have been extensively studied. For instance, Zheng et al. attached Ag nanoparticles onto indium thin oxides (ITOs) by treatment with poly-L-lysine.<sup>14</sup> Cheng et al. connected cetyltrimethylammonium bromide (CTAB)-stabilized Ag nanoparticles to a 3-mercaptopropionic acid modified gold electrode.<sup>15</sup> In addition to the chemical methods, the successful attachment of dispersed Ag nanoparticles onto an ITO surface was reported using a double-pulse electrochemical method.<sup>16</sup> However, the size and dispersed density of the Ag nanoparticles attached to the surfaces are highly dependent on the preparation methods. Also, the characteristics of the Ag-nanoparticle-attached surfaces vary depending on the preparation methods, e.g., are affected by the chemical reagents.

On the other hand, we recently reported a new method to attach Au nanoparticles onto ITO surfaces without using peculiar binder molecules.<sup>17,18</sup> By applying a seed-mediated growth approach that was developed by Murphy and co-workers for the wet chemical synthesis of Au nanorods in aqueous solution,<sup>19,20</sup> Au nanoparticles could be grown on ITO surfaces from the attached seed Au particles.<sup>17,18</sup> In the actual procedure, a piece of the ITO substrate was first immersed in the seed solution containing Au nanoparticles of ca. 3.5-nm diameter and was then immersed in the growth solution containing HAuCl<sub>4</sub>, ascorbic acid, and CTAB. Through this two-step immersion in the solutions, Au-nanoparticle-attached ITO surfaces could be

\* Corresponding author. Tel.: +81-75-753-9152. Fax: +81-75-753-9145. E-mail: oyama@iic.kyoto-u.ac.jp.

<sup>†</sup> Department of Material Chemistry, Graduate School of Engineering.

<sup>‡</sup> Division of Research Initiatives, International Innovation Center.

<sup>§</sup> On leave from Huazhong University of Science and Technology, People's Republic of China.

easily fabricated.<sup>17,18</sup> Compared with conventional Au-nanoparticle-attached ITO electrodes prepared using MPTMS, the electrodes fabricated by the seed-mediated growth method exhibited a lower electron-transfer resistance and more attractive electrochemical and electrocatalytic properties, thus reflecting the absence of binding reagents.<sup>17</sup>

In the present study, we applied this seed-mediated growth method for the fabrication of Ag-nanoparticle-attached ITO surfaces and characterized the properties of the surfaces as electrode materials. The conditions for preparation of a moderately dispersed Ag-nanoparticle-attached ITO surface were established by referring to the conditions for the formation of Ag nanorods and nanowires in solution.<sup>2,3</sup> In particular, the effect of ascorbic acid on the Ag nanostructures formed on the ITO is demonstrated on the basis of surface images recorded using field emission scanning electron microscopy (FE-SEM). In addition, some electrochemical properties of the Ag-nanoparticle-attached ITO surface are presented and compared with those of previously prepared surfaces.<sup>14</sup>

### Experimental Section

**Materials.** Cetyltrimethylammonium bromide (CTAB) and AgNO<sub>3</sub> were purchased from Aldrich Co., Ltd. Trisodium citrate, ascorbic acid, NaBH<sub>4</sub>, NaH<sub>2</sub>PO<sub>4</sub>, Na<sub>2</sub>HPO<sub>4</sub>, K<sub>4</sub>Fe(CN)<sub>6</sub>, K<sub>3</sub>Fe(CN)<sub>6</sub>, and 0.1 M NaOH solution were obtained from Wako Pure Chemicals, Ltd. The ITO film coating on glass plates was ordered from Asahi Beer Optical, Ltd. (resistance, 80  $\Omega$ /mm<sup>2</sup>; size, 18 mm  $\times$  18 mm). A piece of the ITO glass was cut into four pieces and used after being washed in acetone, ethanol, and pure water with sonication and drying with nitrogen gas. In all the procedures, we used pure water prepared using a Millipore Autopure WR600A apparatus (Millipore, Ltd., resistivity > 18 M $\Omega$ ).

**Apparatus.** The size and morphology of the Ag nanoparticles attached to the ITO surface were characterized with field-emission scanning electron microscopy (FE-SEM, JSM-7400F; JEOL, Tokyo, Japan). The electrochemical experiments were performed using 263A potentiostat/galvanostat [Princeton Applied Research (PAR), Oak Ridge, TN] and a 5210 lock-in amplifier (PAR) controlled by a computer with M270 and M398 programs (PAR).

**Procedures.** A seed solution of 4-nm Ag colloid was prepared by the procedure reported by Murphy and co-workers.<sup>2</sup> That is, 0.6 mL of cooled pure water solution of 0.01 M NaBH<sub>4</sub> was added to 20 mL of pure water solution containing 0.25 mM AgNO<sub>3</sub> and 0.25 mM trisodium citrate, and the mixture was maintained for 2 h with stirring. A piece of ITO glass was then immersed into the seed solution and left for 2 h to allow the Ag seed particles to attach to the surface. After the ITO glass had been removed from the seed solution, the ITO surface was washed by being flushed with pure water several times and dried with nitrogen gas.

Following the procedure for making Ag nanowires,<sup>2</sup> in the present study, the growth solution was prepared by mixing the solutions as follows: 0.5 mL of 10 mM AgNO<sub>3</sub> solution, 18 mL of 0.10 M CTAB solution, 0.1 mL of 1.0 M NaOH solution, and typically 0.12 mL of 0.10 M ascorbic acid solution. Whereas the concentration of ascorbic acid after the mixing was 0.64 mM in this case, the effect of the amount of ascorbic acid on the formed Ag nanostructures was examined by changing the added amounts of the ascorbic acid solution to 0.05, 0.08, 0.16, and 0.20 mL; i.e., the final concentrations of ascorbic acid were 0.27, 0.43, 0.86, and 1.06 mM, respectively.

The ITO glass treated in the seed solution was immersed in the growth solution and left for 24 h. This fabricated Ag-

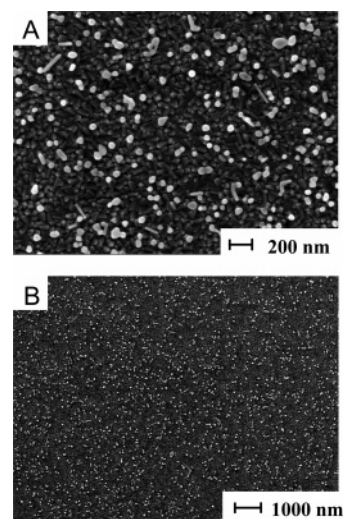


**Figure 1.** FE-SEM images of a Ag-nanoparticle-attached ITO surface. The ITO was first immersed in the seed solution for 2 h and then immersed in a growth solution containing 0.64 mM ascorbic acid for 24 h. (A) Zoomed-in image and (B) zoomed-out image for the same area.

nanoparticle-attached ITO was removed from the growth solution, washed several times with pure water, and then dried for FE-SEM characterization and electrochemical measurements.

### Results and Discussion

**FE-SEM Observation of Ag-Nanoparticle-Attached ITO Surfaces.** First, in Figure 1, we show a typical FE-SEM image of the Ag-nanoparticle-attached ITO surface fabricated using the seed-mediated growth approach. Figure 1A is a zoomed-in image, and Figure 1B is the zoomed-out image. To prepare this surface, the ITO was first immersed in the seed solution and then into the growth solution, in which the concentration of the ascorbic acid was adjusted to 0.64 mM.

As shown in Figure 1B, the Ag nanoparticles could be attached to the ITO surface having a moderate dispersion using the present seed-mediated growth method. Although some nanorods, grown crystals, twin-stuck particles, etc., were observed in the FE-SEM image of Figure 1A, the size of nanosphere particles was not very irregular; i.e., the diameters of the sphere nanoparticles were 45–65 nm. As observed for the Au nanoparticles,<sup>17,18</sup> the formation of nanorods would be evidence that the crystal growth of Ag nanoparticles proceeded relatively freely in solution without being bound by the reagents on the surface. Under the present conditions, the aspect ratio of nanorods formed sparsely was 5–15. Despite some variety in the formed nanoparticles (i.e., nanorods, grown crystals, twin-stuck particles, etc.), the FE-SEM observation of the other parts on the same surface confirmed that the entire surface was evenly modified with the Ag nanoparticles.

Similar to the Au nanoparticles,<sup>17,18</sup> the attachment of Ag nanoparticles was strong enough for practical uses. The nanoparticles were not removed from the ITO surface by several flushings with pure water. In addition, no growth of Ag nanoparticles such as that shown in Figure 1 was observed after just immersion in the seed solution, i.e., before treatment in the growth solution, nor after immersion in only the growth solution. Thus, it can be concluded that the seed-mediated growth procedure is effective and essential to attach Ag nanoparticles to ITO surfaces, which is similar to the case for Au.<sup>17,18</sup>

Although the exact mechanism of the attachment of the Ag seed nanoparticles onto the ITO surface is not clearly understood

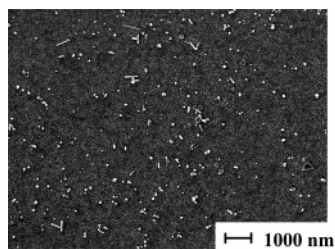


**Figure 2.** FE-SEM image of a Ag-nanoparticle-attached ITO surface. The ITO was first immersed in the seed solution for 2 h and then immersed in a growth solution containing 0.43 mM ascorbic acid for 24 h.

as well as the case for Au nanoparticles,<sup>17,18</sup> the physisorptive properties of the Ag nanocolloids toward the substrate surface are expected to be enhanced in our seeding process. Whereas the aggregation of nanoparticles has been suppressed in the colloid solutions by the capping reagent, i.e., citrate ions in this case, the immersion of heterogeneous material would promote some adsorptive interactions on the surface. In particular, nanoparticles can approach very closely to the surface, so that the interactions between the surface and the negatively charged Ag nanoparticles surrounded by the citrate ions is sufficient to cause the attachment. For example, van der Waals interactions might be possible to form the initial physisorption, and the negative charge of the Ag nanoparticles might cause the fluctuation in the electronic charge distribution in the ITO crystals to form coulombic static binding.

Experimentally, we confirmed that the attachment of the Ag nanoparticles is not peculiar to the ITO surface; they could be attached on the normal glass surface by the same procedures. Thus, we believe that the physisorption of the nanoparticles is promoted to cause the attachment in our treatment, not via special chemical bonding. In addition, our group recently found that “touching” the seed solution with a piece of tissue paper promoted the high-density attachment of Au nanoparticles on ITO surfaces.<sup>21</sup> This would be evidence that the physisorption process is a key interaction in the attachment of the seed nanoparticles. However, because of the resolution of the FE-SEM, the images of the small seed nanoparticles attached on the ITO surface could not be recorded. We discuss the attachment of Ag seed nanoparticles later on the basis of the electrochemical results.

In the growth solution, if CTAB is not present, the reduction of  $\text{Ag}^+$  to Ag proceeds soon after mixing because of the effect of ascorbic acid as a reductant. In other words, the role of CTAB in the proposed method is to suppress the reduction of  $\text{Ag}^+$ , and it has an important function in the formation of nanorods and nanowires in solution.<sup>2,3,19,20</sup> Thus, in the next section, we controlled the power of reduction by changing the amount of ascorbic acid in the growth solution and observed the changes in the surface morphology formed on the ITO surfaces.

**Effect of Ascorbic Acid on Ag Nanostructures Formed on ITO.** When the concentration of ascorbic acid was adjusted to as low as 0.27 mM, no crystal growth of Ag nanoparticles was observed on the ITO surfaces. This means that the reduction power is too weak to promote the crystal growth of Ag when the amount of ascorbic acid in the growth solution is as low as 0.27 mM.

Next, Figure 2 shows a typical FE-SEM image observed after immersion in the seed solution first, followed by immersion into the growth solution containing 0.43 mM ascorbic acid. In this case, the dispersion of the Ag nanoparticles was so sparse that the expanded area was displayed in Figure 2 for comparison

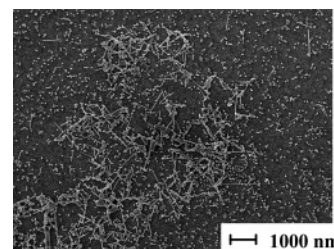


**Figure 3.** FE-SEM image of a Ag-nanoparticle-attached ITO surface. The ITO was first immersed in the seed solution for 2 h and then immersed in a growth solution containing 0.86 mM ascorbic acid for 24 h.

with the image in Figure 1B. Although some crystal growth to form Ag nanorods and larger particles was observed, the grown size of the Ag nanosphere particles was almost identical to that in Figure 1B. That is, as the effect of the reduced amount of ascorbic acid, the Ag nanoparticles were very sparsely formed at a lower density. Thus, it was found that reducing the amount of ascorbic acid effectively reduced the density rather than the size of the formed Ag nanoparticles.

On the other hand, an increase in the ascorbic acid content significantly changed the morphology of the Ag nanoparticles formed on the ITO surfaces. Figure 3 shows a typical FE-SEM image of the ITO surface observed after immersion first in the seed solution and then in the growth solution containing 0.86 mM ascorbic acid. From this image, it is clearly recognized that the formation of Ag nanorods and nanowires was significantly promoted by increasing the amount of ascorbic acid to 0.86 mM. When compared with the image in Figure 2, the size of the Ag nanosphere particles was not very different. In addition, the dispersion of the Ag nanoparticles was not very dense in comparison with the image of Figure 1B. Thus, it is considered that the increased amount of ascorbic acid (from 0.64 to 0.86 mM) was used to promote the one-dimensional growth of the Ag nanorods and nanowires as shown in Figure 3, while the ascorbic acid was utilized at first to increase the attached density of Ag nanoparticles from 0.43 to 0.64 mM. Referring to the regularity on the surface, the gathering parts of the Ag nanorods and nanowires were not as regular as the Ag nanoparticles formed under the conditions of Figure 1B.

A further increase in the amount of ascorbic acid caused more dramatic changes in the surface morphology. Figure 4 shows the FE-SEM images observed after immersion in the growth solution containing 1.06 mM ascorbic acid. Two FE-SEM images having different attaching densities and grown structures are shown in Figure 4. Although some thin Ag nanowires and Ag nanoparticles were observed, the crystals of larger size and irregular shape were recognized in the images. These larger crystals can probably be assigned to the grown Ag particles, because we carefully washed the surface several times before the SEM measurement. When the amount of reducing reagent, i.e., ascorbic acid, is increased, the amount of Ag formed should increase. However, the area uncovered by the small Ag nanoparticles becomes significant under these conditions compared with previous ones. Thus, it is inferred that the Ag nanoparticles gathered and aggregated to form larger crystals in the growth solution. Under these conditions, the attachment of the Ag nanoparticles cannot be described as a “regular dispersion”.

As shown in the FE-SEM images of Figure 4, the formed structures and density of the Ag nanoparticles on the ITO surfaces were highly sensitive to the concentration of ascorbic acid in the growth solution. Whereas the present results demonstrate dramatic changes in the Ag nanostructures, a fine-tuning of the concentration of ascorbic acid should effectively



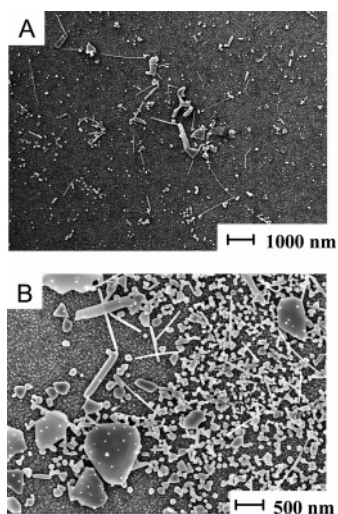


**Figure 4.** FE-SEM images of the Ag-nanoparticle-attached ITO surface: Ag nanoparticles (A) in a sparsely formed area and (B) in a densely formed area. The ITO was first immersed in the seed solution for 2 h and then immersed in a growth solution containing 1.06 mM ascorbic acid for 24 h.

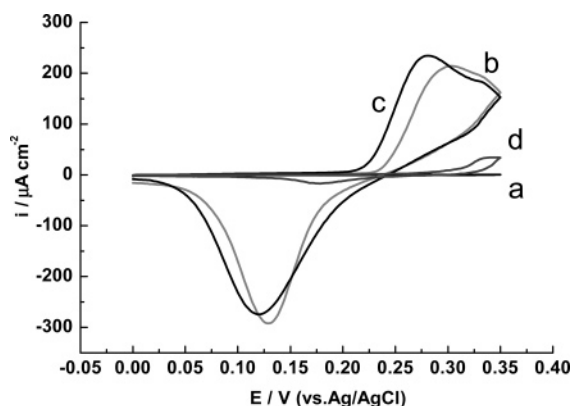


**Figure 5.** Cyclic voltammograms of the oxidation processes in 0.1 M  $\text{KNO}_3$  aqueous solution recorded using (a) bare ITO electrode, (b) conventional Ag electrode, (c) AgNP/ITO electrode, and (d) AgSD/ITO electrode. Scan rate:  $50 \text{ mV s}^{-1}$ . The current axis was normalized by dividing by the surface areas in contact with the solutions.

control the attached density and surface morphology of the Ag nanoparticles to some extent.

**Electrochemical Characterization of Ag-Nanoparticle-Attached ITO Surface.** To evaluate the electrochemical properties of the Ag-nanoparticle-attached ITO (AgNP/ITO), several electrochemical measurements were carried out using the ITO surfaces as working electrodes. For this purpose, the ITO was connected to a strip of copper adhesive tape and then molded onto a piece of scotch tape that was made to have a 2-mm-diameter hole. For the electrochemical measurement, the exposed area of  $\phi = 2.0 \text{ mm}$  contacted the solution.

In the present study, we observed the electrochemical properties of AgNP/ITO samples prepared under the conditions used to give the surface images in Figure 1, because some irregularity in the Ag nanoparticles occurred at higher ascorbic acid concentrations, as described in the previous section. In addition, for comparison, we used a Ag-seed-modified ITO (AgSD/ITO) electrode that was prepared by immersing an ITO substrate only in the seed solution for 2 h.

First, the oxidation and reduction properties of the AgNP/ITO were examined in 0.1 M  $\text{KNO}_3$  solution. Figure 5 shows the electrochemical response of the AgNP/ITO surface together

with those of a bare ITO electrode, a normal Ag electrode (BAS Co., Ltd.,  $\phi = 1.6 \text{ mm}$ ), and the AgSD/ITO electrode. The current values were normalized in units of  $\mu\text{A cm}^{-2}$ .

A redox response (Figure 5b) was observed with the polished normal Ag electrode, whereas no current response was observed on the bare ITO electrode (Figure 5a). This response (Figure 5b) can be attributed to the oxidation of Ag and the reduction of silver oxides on the surface. Because a very similar response was observed on the AgNP/ITO electrode (Figure 5c), it is apparent that the redox behavior of Ag nanoparticles manifested itself in the cyclic voltammogram.

However, in addition to the verification of the presence of Ag, two specific conclusions can be drawn as follows:

(1) The normalized current value of the AgNP/ITO electrode is almost the same as that of the Ag electrode, which means that the amount of the Ag nanoparticles oxidized is similar to the amount for the polished Ag electrode. Because the area covered by the Ag nanoparticles was ca. 17% in the FE-SEM image in Figure 1, the current observed with the AgNP/ITO electrode is apparently larger than that expected from the outer surfaces of Ag nanoparticles even though we assume the three dimensional expansion. Thus, some promotion of the oxidation is expected for the Ag nanoparticles compared with the polished Ag surface.

(2) If oxidation had promoted the dissociation of Ag nanoparticles from the ITO surface in the AgNP/ITO electrode, the shape of the current response (c) would have been different from response b. However, the redox behaviors were essentially the same. Thus, the Ag nanoparticles are expected to strongly attach to the ITO surface for the electrochemical measurements with a good junction and high conductivity, and consequently, the outer surfaces of the Ag nanoparticles are considered to be involved in an electrochemical response similar to that of the normal Ag electrode.

The steeper increase in the oxidation current of the AgNP/ITO electrode (Figure 5c) compared with that of the Ag electrode (Figure 5b) also supports the high conductivity and strong connection between the Ag nanoparticles and the ITO surface.

On the other hand, on the AgSD electrode, a smaller but recognizable electrochemical response was observed, as shown in Figure 5d. In this case, the consumed charge in the oxidation was ca. 0.15 mC, which was smaller than that of the AgNP electrode (2.5 mC). However, if this value corresponds to the outer surface area of the Ag nanoparticles, the difference in the consumed charge should be much more significant. For this point, because a potential shift and a shape change were observed in response d compared with the response c, a simple comparison of the area seems to be difficult from the electrochemical responses.

**Electrochemical Impedance of Ag-Nanoparticle-Attached ITO Surface.** The electrochemical impedance of the AgNP/ITO electrode surface was next measured to evaluate the effects of the Ag nanoparticles on the electron-transfer reactions. We compared the electron-transfer resistance values among the bare ITO, AgNP/ITO, and AgSD/ITO electrodes. Figure 6 shows Cole–Cole plots for the three electrodes for a solution containing  $[\text{Fe}(\text{CN})_6]^{3-}$  and  $[\text{Fe}(\text{CN})_6]^{4-}$ . From the obtained results, the charge-transfer resistivity ( $R_{ct}$ ) values could be determined to be 2.39, 1.54, and 1.04  $\text{k}\Omega/\text{cm}^2$  for the bare ITO, AgSD/ITO, and AgNP/ITO electrodes, respectively.

Although the Ag seed particles were not observed in the FE-SEM measurements as mentioned before, the results of the electrochemical impedance measurements showed a significant effect due to the attachment of the Ag seed nanoparticles as well as the grown Ag nanoparticles. For the Au nanoparticles,

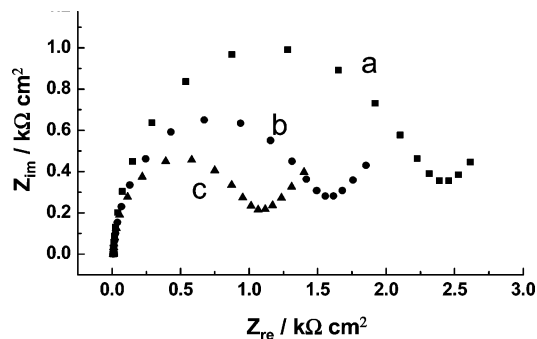


**Figure 6.** Electrochemical impedance spectra recorded at 0.22 V in 0.1 M phosphate buffer solution (pH 7.0) containing 0.5 mM  $[\text{Fe}(\text{CN})_6]^{3-}$  and 0.5 mM  $[\text{Fe}(\text{CN})_6]^{4-}$  using (a) bare ITO electrode, (b) AgSD/ITO electrode, and (c) AgNP/ITO electrode.

the reduction of the  $R_{ct}$  value of the AuSD/ITO electrode from that of the bare ITO was ca. 0.12  $\text{k}\Omega/\text{cm}^2$ . Therefore, a significant effect of the Ag seed nanoparticles on electron transfer can be recognized from the present data.

**Electrochemical Behavior of  $[\text{Fe}(\text{CN})_6]^{3-}/[\text{Fe}(\text{CN})_6]^{4-}$  on Ag-Nanoparticle-Attached ITO Surface.** Because the changes in the  $R_{ct}$  value could be confirmed, the redox responses of  $[\text{Fe}(\text{CN})_6]^{3-}/[\text{Fe}(\text{CN})_6]^{4-}$  in 0.1 M phosphate buffer solution (pH 7.0) were observed using bare ITO, AgSD/ITO, and AgNP/ITO electrodes. The results are shown in Figure 7a–c. As can be seen, a much improved reversible behavior was observed with the AgNP/ITO electrodes (Figure 7c), and the AuSD/ITO electrode also gave a slightly improved response (Figure 7b). The peak separation values were 418, 352, and 240 mV for the bare ITO, AuSD/ITO, and AgNP/ITO electrodes, respectively.

However, it might be thought strange that the redox response of Ag was not observed in Figure 7c despite the overlapping in the potential range with the redox response of Ag itself as in Figure 5. Actually, the redox response of the AgNP/ITO electrode in 0.1 M phosphate buffer in the absence of  $[\text{Fe}(\text{CN})_6]^{3-}/[\text{Fe}(\text{CN})_6]^{4-}$  exhibited the oxidation and reduction of AgNP on the ITO with significant current values as shown in Figure 7d.

The difference between voltammograms c and d of Figure 7 can be explained in terms of the effect of the Ag nanoparticles on electron transfer. In the result of Figure 7c, it is considered that the Ag nanoparticles promote the electron transfer of  $[\text{Fe}(\text{CN})_6]^{3-}/[\text{Fe}(\text{CN})_6]^{4-}$  by existing on the *conducting* ITO surface and that the oxidation of Ag is suppressed. In contrast, in the absence of  $[\text{Fe}(\text{CN})_6]^{3-}/[\text{Fe}(\text{CN})_6]^{4-}$  (Figure 7d), the Ag nanoparticles have to be involved in the redox reactions. Thus, the present result of Figure 7c can be regarded as a good expression of the function of Ag nanoparticles in promoting electron transfer. Actually, on the conventional Ag disk electrode, we could not observe the reversible behavior of the  $[\text{Fe}(\text{CN})_6]^{3-}/[\text{Fe}(\text{CN})_6]^{4-}$  couple, but rather observed the redox response of Ag.

Judging from the present results, it is apparent that first the Ag seed nanoparticles attached to the ITO surface upon immersion of the ITO into the seed solution, and then the Ag nanoparticles grew from the seed particles in the growth solution. Similar to the case of Au,<sup>19,20</sup> it is inferred that the small Ag seed nanoparticles (4 nm) capped by the citrates become the adhesive to the ITO surface, and that the Ag nanoparticles grow from the seed particles while being protected by CTA<sup>+</sup>. As a characteristic feature of the seed-mediated growth approach without using peculiar binding reagents, the  $R_{ct}$  values could be significantly lowered using Ag nanoparticles, as was also the case for Au nanoparticles.<sup>17</sup>

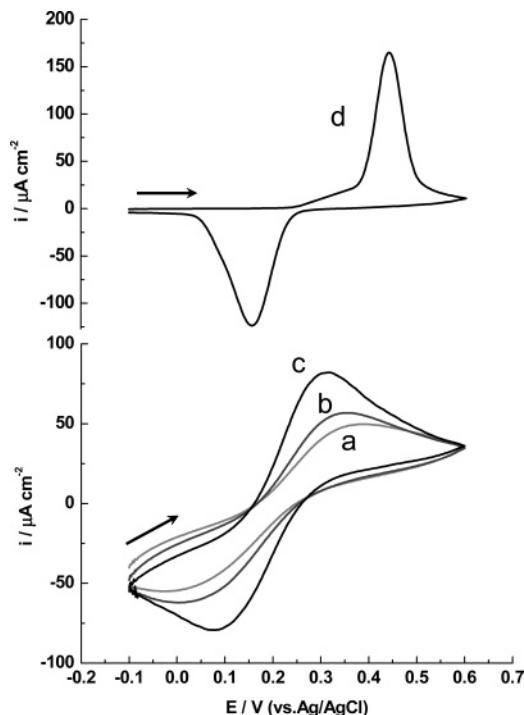


**Figure 7.** Cyclic voltammograms of 0.5 mM  $[\text{Fe}(\text{CN})_6]^{3-}$  and 0.5 mM  $[\text{Fe}(\text{CN})_6]^{4-}$  in 0.1 M phosphate buffer solution (pH 7.0) recorded using (a) bare ITO electrode, (b) AgSD/ITO electrode, and (c) AgNP/ITO electrode. Scan rate: 50  $\text{mV s}^{-1}$ . The current axis was normalized by dividing by the surface areas in contact with the solutions. (d) Cyclic voltammogram recorded using AgNP/ITO electrode for 0.1 M phosphate buffer solution (pH 7.0) in the absence of  $[\text{Fe}(\text{CN})_6]^{3-}/[\text{Fe}(\text{CN})_6]^{4-}$  couple.

**Electroreduction Behaviors of  $\text{MV}^{2+}$  on Ag-Nanoparticle-Attached ITO Surfaces.** Zheng et al. compared the surface properties of an electrochemically roughened Ag surface and an assembled Ag nanoparticles/ITO (AAgNP/ITO) surface that was fabricated using poly-L-lysine.<sup>14</sup> Using the electrochemical responses during the reduction of methyl viologen dication ( $\text{MV}^{2+}$ ) and the SERS spectra, it was clearly shown that  $\text{MV}^{2+}$  was strongly adsorbed on the surface of the roughened Ag but not on the surface of their AAgNP/ITO electrode. In the latter case, a beautiful reversible response was shown for the reduction of  $\text{MV}^{2+}$ , whereas the reduction wave of the adsorbed  $\text{MV}^{2+}$  was observed in the positive potential region for the roughened Ag surface.<sup>14</sup>

Thus, we tried to observe the reduction behavior of  $\text{MV}^{2+}$  on the surface of our AgNP/ITO electrode to investigate the differences in the adsorption of  $\text{MV}^{2+}$ . Figure 8c shows the cyclic voltammogram of  $\text{MV}^{2+}$  observed on the AgNP/ITO electrode, together with the voltammograms for the (a) bare ITO and (b) polished Ag electrodes. Whereas a quasireversible response was observed on the bare ITO electrode (Figure 8a), prewaves and distortion were observed on the AgNP/ITO electrode (Figure 8c), which implied the adsorption of  $\text{MV}^{2+}$  on the Ag nanoparticles. That is, although no adsorption of  $\text{MV}^{2+}$  was clearly shown on the previous AAgNP/ITO electrode,<sup>14</sup> the adsorption was recognized on the present AgNP/ITO electrode.

As a possible reason for this difference, we point out that the binder molecules would affect the nature of the formed nanoparticles, as clearly shown in the case of Au,<sup>18</sup> and additionally, they might affect the surface properties. Because poly-L-lysine, which has positive charges, was used for the preparation of the AAgNP/ITO electrode,<sup>14</sup> the positive charges

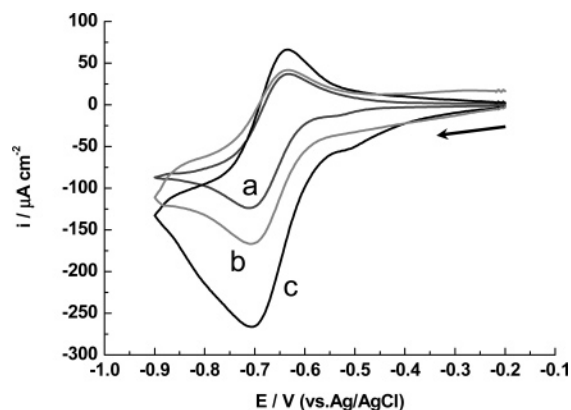


**Figure 8.** Cyclic voltammograms of 0.5 mM methyl viologene dication in 0.1 M  $\text{Na}_2\text{SO}_4$  recorded using (a) bare ITO electrode, (b) conventional Ag electrode, and (c) AgNP/ITO electrode. Scan rate:  $100 \text{ mV s}^{-1}$ . The current axis was normalized by dividing by the surface areas in contact with the solutions.

will possibly repel  $\text{MV}^{2+}$  from the surface. In contrast, because the Ag nanoparticles were directly attached without using binder molecules in our method, it is expected that adsorption on the outer surfaces of the Ag nanoparticles is possible. At any rate, it is true that a Ag-nanoparticle-attached ITO surface having different electrochemical properties has been fabricated using the different approach in the present work, compared with the previous one.<sup>14</sup>

In our result, Figure 8c shows a large current response compared to those of the ITO electrode (Figure 8a) and the Ag electrode (Figure 8b). This is due to the fact that both the bare ITO area and the Ag nanoparticles on the AgNP/ITO work as the electrode for the  $\text{MV}^{2+}$  reduction, which is different from the case of  $[\text{Fe}(\text{CN})_6]^{3-}/[\text{Fe}(\text{CN})_6]^{4-}$ . A simple estimation showed that the redox peak currents of Figure 8c could be predicted by assuming the contributions of 45% of the response of the ITO electrode (Figure 8a) and 120% of the Ag electrode (Figure 8b). For this result, the contribution of the ITO electrode might be thought to be smaller than the value expected from the FE-SEM image of Figure 1A (the surface area of the bare ITO area in Figure 1A was ca. 83%). However, in this case, the redox response of the Ag electrode also included the reversible reaction of the  $\text{MV}^{2+}$  in solution. Thus, the values of the contributions seem to be appropriate judging from the overlapping of the expected diffusion layer around the Ag nanoparticles with that of the ITO surface and the result that the oxidative currents were almost the same for the Ag and AgNP/ITO electrodes (Figure 5).

In this case, the electron-transfer reactions on the bare parts of the ITO surface should be taken into account in a discussion of the electrochemical responses. This might become a disadvantage in analyzing the electrochemical responses compared with the conventional metal nanoparticle attachment methods, in which the electron-transfer reactions tend to be shielded by the binder reagents. However, if we can utilize the differences in the electrochemical characteristics between Ag nanoparticles and ITO, it might be possible to construct a unique nanoelectrode to exhibit both of these characters.

## Conclusions

In the present study, we fabricated Ag-nanoparticle-attached ITO surfaces using the seed-mediated growth approach. Similar to our previous results of the Au nanoparticles,<sup>17,18</sup> it is considered that the small Ag seed nanoparticles capped by citrates easily become attached to the ITO surface and that the Ag nanoparticles grow from the seed particles protected by  $\text{CTA}^+$ .

For Ag, a moderately dispersed AgNP/ITO surface could be prepared, as shown in Figure 1, by the careful adjustment of the amount of ascorbic acid in the growth solution. It is interesting that an increase in the amount of ascorbic acid promoted the formation of Ag nanorods and nanowires, rather than an increase in the attached density of the Ag nanoparticles.

The electrochemical results showed that the Ag nanoparticles were attached strongly enough for use as a working electrode. Because the oxidative electrochemical response showed the oxidation of Ag on the outer surfaces of the nanoparticles, and not the oxidative desorption of nanoparticles, it is inferred that the electrical contact between the Ag nanoparticles and the ITO surface should be strong. In addition, a decrease in  $R_{\text{ct}}$  due to the growth of Ag nanoparticles was confirmed by the impedance measurement, even though only the Ag seed nanoparticles could also reduce the  $R_{\text{ct}}$  value. This is a characteristic feature of the proposed method without the use of binding molecules. As another possible manifestation of the AgNP/ITO electrode fabricated without using binder molecules, the adsorption of  $\text{MV}^{2+}$  was observed during the electrochemical reduction.

Although the fabrication of the AgNP/ITO and electrochemical evaluations have been reported in this present study, further studies utilizing the present AgNP/ITO electrode, e.g., for SERS measurements and electrocatalytic properties, are now in progress.

**Acknowledgment.** This work was supported by the Kyoto Nanotechnology Cluster Project, a Grant for Regional Science and Technology Promotion from the Ministry of Education, Culture, Sports, Science and Technology, Japan. J.Z. is grateful for the postdoctoral fellowship from the same grant. G.C. thanks the Monbukagakaku-sho scholarship as a doctoral course student at Kyoto University. The authors also thank the Kyoto University Venture Business Laboratory (KU-VBL) Project.

## References and Notes

- (1) Sun, Y.; Xia, Y. *Science* **2002**, 298, 2176.
- (2) Jana, N. R.; Gearheart, L.; Murphy, C. J. *Chem. Commun.* **2001**, 617.
- (3) Murphy, C. J.; Jana, N. R. *Adv. Mater.* **2002**, 14, 80.
- (4) Sun, Y.; Gates, B.; Mayers, B.; Xia, Y. *Nano Lett.* **2002**, 2, 165.
- (5) Sun, Y.; Xia, Y. *Adv. Mater.* **2002**, 14, 833.
- (6) Yin, B.; Ma, H.; Wang, S.; Chen, S. *J. Phys. Chem. B* **2003**, 107, 8898.
- (7) Jiang, L.-P.; Wang, A.-N.; Zhao, Y.; Zhang, J.-R.; Zhu, J.-J. *Inorg. Chem. Commun.* **2004**, 7, 506.
- (8) Freeman, R. G.; Grabar, K. C.; Allison, K. J.; Bright, R. M.; Davis, J. A.; Guthrie, A. P.; Hommer, M. B.; Jackson, M. A.; Smith, P. C.; Walter, D. G.; Natan, M. J. *Science* **1995**, 267, 1629.
- (9) Chumanov, G.; Sokolov, K.; Gregory, B. W.; Cotton, T. M. *J. Phys. Chem.* **1995**, 99, 9466.
- (10) Bright, R. M.; Musick, M. D.; Natan, M. J. *Langmuir* **1998**, 14, 5695.
- (11) McFarland, A. D.; Van Duyne, R. P. *Nano Lett.* **2003**, 3, 1057.
- (12) Rondinini, S. B.; Mussini, P. R.; Crippa, F.; Sello, G. *Electrochem. Commun.* **2000**, 2, 491.
- (13) Dai, J.; Bruening, M. L. *Nano Lett.* **2002**, 2, 497.
- (14) Zheng, J.; Li, X.; Gu, R.; Lu, T. *J. Phys. Chem. B* **2002**, 106, 1019.
- (15) Cheng, W.; Dong, S.; Wang, E. *Electrochem. Commun.* **2002**, 4, 412.
- (16) Sandmann, G.; Dietz, H.; Plieth, W. *J. Electroanal. Chem.* **2000**, 491, 72.
- (17) Zhang, J.; Kambayashi, M.; Oyama, M. *Electrochem. Commun.* **2004**, 6, 683.
- (18) Kambayashi, M.; Zhang, J.; Oyama, M. *Cryst. Growth Des.*, **2005**, 5, 81.
- (19) Jana, N. R.; Gearheart, L.; Murphy, C. J. *J. Phys. Chem. B* **2001**, 105, 4065.
- (20) Busbee, B. D.; Obare, S.; Murphy, C. J. *Adv. Mater.* **2003**, 15, 414.
- (21) Ali Umar, A.; Oyama, M. *Cryst. Growth Des.*, published online Nov. 13, <http://dx.doi.org/10.1021/cg049711p>.